Journal of Neuroscience Methods 363 (2021) 109348

Contents lists available at ScienceDirect

Journal of Neuroscience Methods

journal homepage: www.elsevier.com/locate/jneumeth

Bringing together the best of chemistry and biology: hybrid indicators for imaging neuronal membrane potential

Shuzhang Liu [a,1], Junqi Yang [b,1], Peng Zou [a,c,d,*]

[a] College of Chemistry and Molecular Engineering, Synthetic and Functional Biomolecules Center, Beijing National Laboratory for Molecular Sciences, Key Laboratory of Bioorganic Chemistry and Molecular Engineering of Ministry of Education, Peking University, Beijing 100871, China
[b] Peking-Tsinghua-NIBS Joint Graduate Program, Peking University, Beijing 100871, China
[c] PKU-IDG/McGovern Institute for Brain Research, Peking-Tsinghua Center for Life Sciences, Peking University, Beijing 100871, China
[d] Chinese Institute for Brain Research (CIBR), Beijing 102206, China

A B S T R A C T

Membrane potential is an indispensable biophysical signal in neurobiology. Imaging neuronal electrical signals with fluorescent indicators allows for non-invasive recording at high spatial resolution. Over the past decades, both genetically encoded voltage indicators (GEVIs) and organic voltage sensing dyes (OVSDs) have been developed to achieve imaging membrane potential dynamics in cultured neurons and in vivo. More recently, hybrid voltage indicators have gained increasing attention due to their superior fluorescent quantum yield and photostability as compared to conventional GEVIs. In this mini-review, we summarize the design, characterization and biological applications of hybrid voltage indicators, and discuss future improvements.

1. Introduction

Membrane potential is a ubiquitous biophysical property in cell biology. In excitable cells, such as neurons, membrane potential is intricately regulated to achieve long distance electrical signaling: a neuron integrates its excitatory and inhibitory synaptic inputs into all-or-none action potential (AP) spikes. Conventionally, membrane potentials could be measured by electrode-based techniques, including whole-cell patch clamp and extracellular recording. While patch clamp has remained as the gold standard for electrophysiology owing to its sub-millivolt sensitivity and sub-millisecond temporal resolution, it nevertheless suffers from high invasiveness, lack of sufficient spatial resolution and limited multiplicity in terms of simultaneously recording from a large number of neurons (Lazzari-Dean et al., 2021). The development of microelectrode probes such as ultrathin CMOS array has dramatically increased measurement throughput by at least three orders of magnitude (Shahrjerdi and Bedell, 2013). For instance, Neuropixels 2.0 probe offers more than 5000 recording sites along four narrow shanks (~1 cm per shank) (Steinmetz et al., 2021). However, as with other extracellular recording techniques, microelectrode arrays often provide only spike timing information but fail to report sub-threshold voltage changes.

Voltage imaging in neurons offers another exciting avenue for measuring membrane potential dynamics with high spatial and temporal resolutions. For this purpose, organic voltage sensitive dyes (OVSDs) have been synthesized to visualize AP spikes in cultured neurons, brain slices and in vivo (Miller, 2016). A major drawback of OVSDs is their high lipophilicity, which hinders cell-specific targeting and causes high fluorescence background in the tissue. Genetically encoded voltage indicators (GEVIs) can be expressed in specified cell types and even subcellular compartments, thus substantially reducing background staining in a dense cell population (Adam et al., 2019). However, the photophysics of fluorescent proteins (FPs) in GEVIs are often inferior to synthetic dyes, in terms of both molecular brightness and photobleaching rate (Lavis and Raines, 2008; Wang et al., 2018). To overcome the above limitations, several hybrid strategies have been developed to combine the advantages of genetic expression with the remarkable photophysical properties of synthetic dyes (Fig. 1). Depending on their structures and design principles, existing hybrid voltage sensors could be broadly divided into two classes: protein-targeted OVSDs to achieve cell-specific labeling, and dye-modified GEVIs to improve the photophysics of fluorescence reporters. In this mini-review, we discuss the design, characterization and biological applications of these hybrid indicators.

* Corresponding author at: College of Chemistry and Molecular Engineering, Synthetic and Functional Biomolecules Center, Beijing National Laboratory for Molecular Sciences, Key Laboratory of Bioorganic Chemistry and Molecular Engineering of Ministry of Education, Peking University, Beijing 100871, China.
E-mail address: zoupeng@pku.edu.cn (P. Zou).
[1] These authors contributed equally to this work.

https://doi.org/10.1016/j.jneumeth.2021.109348
Received 25 May 2021; Received in revised form 27 August 2021; Accepted 30 August 2021
Available online 2 September 2021
0165-0270/© 2021 Published by Elsevier B.V.

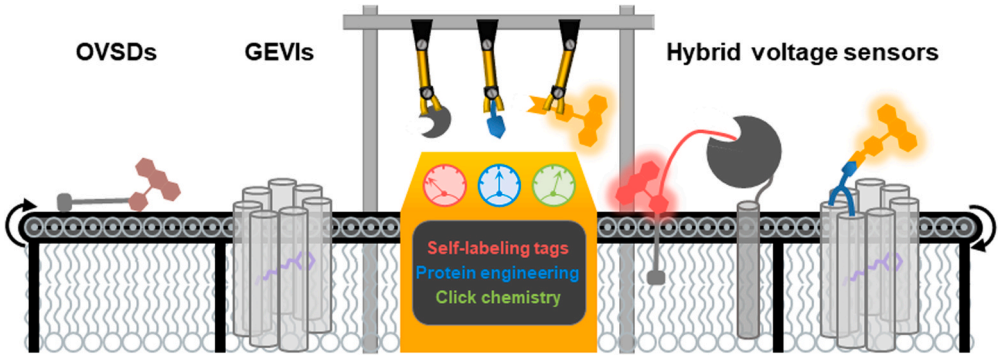

Fig. 1. Scheme of basic strategies for "processing" an OVSD or a GEVI into a hybrid "product" with cell specificity and remarkable photophysical properties.

2. OVSD-derived hybrid voltage sensors

Depending on their voltage-sensing mechanisms, OVSDs typically fall into four categories: solvatochromic dyes, electrochromic dyes, voltage-dependent redistribution dyes, and photoinduced electron transfer (PeT) dyes (Miller, 2016; Kulkarni and Miller, 2017). Hybrid strategies have been applied to each category to overcome indiscriminative staining.

2.1. Solvatochromic dyes

A solvatochromic dye is characterized by exhibiting enhanced fluorescence emission when entering less polar solvent. Such environment-sensitive fluorescence enhancement could be also observed when the dye is partitioned into the hydrophobic cellular membrane, as exemplified by Merocyanine 540 (Fig. 2A), which was developed by Cohen and co-workers in the 1970s. Upon membrane depolarization, the negatively charged Merocyanine 540 accumulates in cell membrane due to electrostatic interactions and emits more intensely. As one of the earliest OVSDs, Merocyanine 540 could report APs in a giant axon of squid with $\Delta F/F_0$ of 0.1% (Davila et al., 1973). Since then, a broad palette of OVSDs have been developed (Sundukova et al., 2019; Yan et al., 2012).

Nile Red (Fig. 2A) is another solvatochromic dye that exhibits a voltage sensitivity of − 5.1% $\Delta F/F_0$ per 100 mV. To achieve cell-specific targeting, Nile Red is conjugated with coenzyme A, which can be conjugated with a GPI-anchored 8 kDa protein, acyl carrier protein (ACP)-tag (Fig. 2B). The resulting hybrid sensor, termed STeVI1 (semisynthetic tethered voltage indicator 1), could report APs in targeted neurons with a sensitivity of − 2.2% $\Delta F/F_0$ per AP (Table 1) (Sundukova et al., 2019).

2.2. Electrochromic dyes

Membrane-embedded electrochromic dyes respond to membrane potential changes through Stark effect, in which the interaction between the dye molecule's electric dipole and external electric field shifts the energy levels of its electronic ground state and excited state. Consequently, the absorption and emission spectra of an electrochromic dye would quickly respond to changes in the membrane potential, typically with a spectral shift of less than 10 nm. For instance, the electrochromic hemicyanine dye, di-4-ANEPPS (Fig. 2A), has a sensitivity of − 10% $\Delta F/F_0$ per 100 mV at 610 nm (Fluhler et al., 1985).

Genetic targeting of electrochromic dyes has been achieved with enzymatic activation. For example, di-4-ANEPPS was modified with two phosphonooxymethyl-ammonium zwitterions. This OVSD precursor could not insert into the cell membrane until being dephosphorylated by a phosphatase displayed on the cell surface (Fig. 2B). The activated di-4-ANEPPS is voltage sensitive (− 10% $\Delta F/F_0$ per 100 mV), but has not been shown to report AP in neurons (Table 1) (Ng and Fromherz, 2011). Since the dynamic range of electrochromic dyes are dependent on the imaging wavelength, it is often important to carefully choose the bandwidth of emission filters to maximize the detection sensitivity. Detecting near the edge of the spectra yields much higher sensitivity than detecting near the peak.

2.3. Voltage-dependent redistribution dyes

Voltage-dependent redistribution dyes are cell membrane-embedded, negatively charged lipophilic molecules, which translocate between the inner and outer leaflets of the lipid bilayer in response to changes in the membrane potential. These dyes could act as fluorescence quenchers and are often paired with a membrane anchored fluorescence donor to achieve voltage-dependent modulation of Förster resonance energy transfer (FRET) quenching efficiency. For example, Tsien and co-workers used a phospholipid-modified coumarin as the donor and a membrane-embedded oxonol as the acceptor to develop a voltage sensor with a sensitivity of 50% $\Delta F/F_0$ per 100 mV (Gonzalez and Tsien, 1997). Similarly, the lipophilic anion quencher dipicrylamine (DPA) was paired with the membrane-targeted fluorophore DiO to achieve a voltage sensitivity of − 56 ± 3% $\Delta F/F_0$ per 100 mV (Bradley et al., 2009).

To achieve cell-specific targeting, the synthetic fluorescence donor (e.g. DiO) was replaced with genetically targetable FPs (e.g. membrane-localized EGFP) (Chanda et al., 2005). Using farnesylated EGFP as the donor and DPA as the acceptor (Fig. 2B), the resulting hybrid voltage sensor (hVOS) could detect voltage signals from cultured neurons with a sensitivity of − 4.2% $\Delta F/F_0$ per AP (Table 1) (Chanda et al., 2005) Through a combination of FP engineering, linker optimization and membrane targeting motif screening, an improved version (hVoS 2.0) was developed to achieve a sensitivity of − 10% $\Delta F/F_0$ per AP in cultured neurons (Fig. 2C and Table 1) (Wang et al., 2010). In 2017, hVoS 2.0 was applied to voltage imaging in mouse brain slices, where it reported AP waveforms from distinct neuronal subtypes and captured the differences in response latencies from neighboring neuronal populations. Such information could be helpful to identify the connectivity within the neural network. At the subcellular level, voltage imaging with hVoS 2.0 offers sufficient spatial-temporal resolution to reveal the propagation of AP across cellular compartments (Bayguinov et al., 2017).

A common drawback of voltage-dependent redistribution strategy is its slow response kinetics, owing to the required migration of molecules inside the membrane. Besides, the charged quenching group embedded within the membrane will increase cell membrane capacitance, which often results in the decreased neuronal excitability. This perturbation on neuronal electrophysiology is particularly evident for DPA, whose concentration has to be carefully controlled to not exceed 3 μM (Sjulson and Miesenbock, 2008). Recently, an azo-benzene dye quencher, termed Disperse Orange3 (D3), was identified as being less toxic in cells and acute brain slices (Alich et al., 2021). D3 replaced DPA as the quencher for membrane-anchored EGFP (GPI-EGFP), and the resulting dqGEVI (dark quencher GEVI) could detect neuronal APs with − 5.0% $\Delta F/F_0$

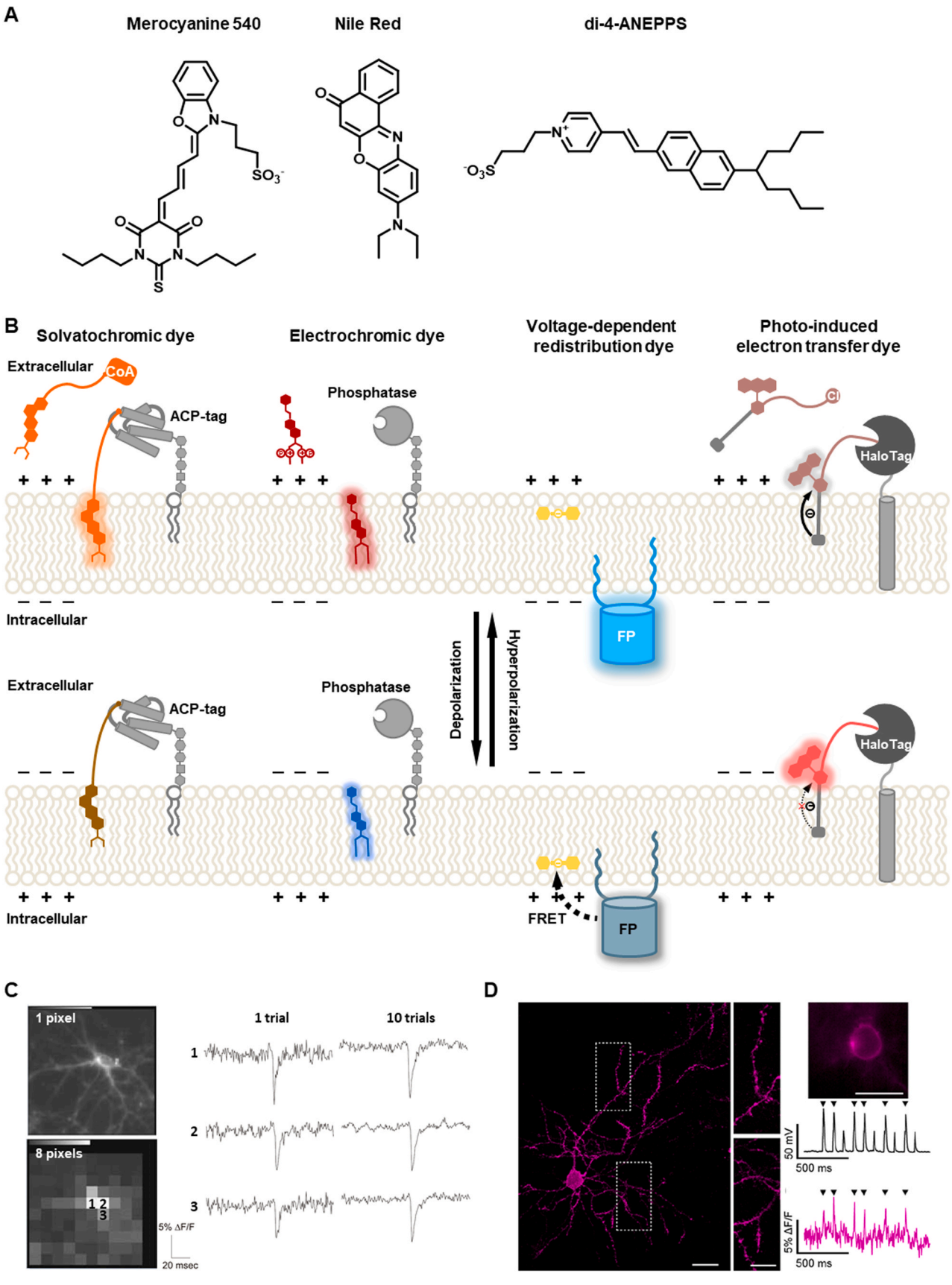

(caption on next page)

Fig. 2. OVSD-derived hybrid voltage sensors. (A) Chemical structures of representative organic voltage sensitive dyes (OVSDs): Merocyanine 540 (Davila et al., 1973), Nile Red (Sundukova et al., 2019), and Di-4-ANEPPS (Fluhler et al., 1985). (B) Voltage sensing mechanisms of OVSD-derived hybrid sensors. From left to right: a hybrid solvatochromic dye is conjugated with coenzyme A, which is recognized by the acyl carrier protein (ACP)-tag (Sundukova et al., 2019); a hybrid electrochromic dye precursor is locally uncaged by cell membrane-targeted phosphatase; a hybrid voltage-dependent redistribution dye usually acts as a dark quencher, whose distribution within the cell membrane is regulated by membrane potentials, thus modulating the quenching efficiency of the targeted FP; a hybrid photoinduced electron transfer (PeT) dye is derivatized with a HaloTag ligand, which could be covalently linked to cell membrane-targeted HaloTag. Photoinduced electron transfer through the molecular wire is modulated by the direction and intensity of the transmembrane electric field. (C) hVoS 2.0 reports action potential in cultured neurons (Wang et al., 2010). (D) A maximum projection of z-stack imaged for RhoVR with two photo microscopy, voltage imaging for spike train in a mouse cortical brain slice (Deal et al., 2020).

Table 1
Summary of existing voltage indicators.

Name	Voltage sensing mechanism	Sensitivity $\Delta F/F_0$ (%)		SNR	Illum. intensity (W/cm^2)	Camera frame rate (Hz)	Response kinetics (ms)		Em. peak (nm)	Ext. coeff. ε ($M^{-1}cm^{-1}$)	Q. Y.[b] Φ	R.B.[c]	Ref.
		100 mV	AP[a]	AP[a]			τ_{on}	τ_{off}					
STeVI1	Salvatochromic	-4.9	-2.2	16.2	1.2	770	1.9	1.9	581	38,000	0.7	0.793	(Fluhler et al., 1985)
di-4-ANEPPS precursor	Electrochromism[d]	-10.1	N.A.	N.A.	N.A.	40	N.A.	N.A.	632	N.A.	n.d	n.d	(Ng and Fromherz, 2011)
hVOS	VDRD[e]	-5 to − 34	-4.2	N.A.	N.A.	N.A.	0.53	N.A.	507	55,900	0.6	1.000	(Chanda et al., 2005)
hVoS 2.0	VDRD[e]	-20	-10	N.A.	N.A.	2000	< 0.5	< 0.5	475	43,000	0.62	0.795	(Wang et al., 2010)
dqGEVI	VDRD[e]	-6.6	-5.0	18	0.43	1080/ 2225	N.A.	N.A.	507	55,900	0.6	1.000	(Alich et al., 2021)
VF-EX 2	PeT dye	21	7.3	20	N.A.	500	< 1	< 1	540	98,000	0.013	0.038	(Liu et al., 2017)
carboVF-EX 1	PeT dye	18	8.4	12	N.A.	500	< 1	< 1	593	N.A.	0.001	n.d	(Ortiz et al., 2019)
VoltageSpy 22 (PEG_{35})	PeT dye	12.7	9.7	7.7	0.8	1000	< 1	< 1	546	N.A.	0.087	n.d	(Grenier et al., 2019)
RhoVR1-PEG_{25}-Halo	PeT dye	34	11.1	16.5	1.73–9.73	500	< 1	< 1	585	74,000	0.05	0.110	(Deal et al., 2020)
isoBeRST-Halo 7	PeT dye	21	10	15	1.94	500	< 1	< 1	677	N.A.	0.042	0.094	(Ortiz et al., 2020)
VSD-HaloTag-TMR	VSD	-2	N.A.	N.A.	N.A.	N.A.	slow	slow	574	92,000	0.1	0.274	(Tsutsui et al., 2013)
$HArcLight_{635}$	VSD	-3.5	-3	N.A.	N.A.	400	2.2	1.6	656	81,000	0.75	1.811	(Deo et al., 2021)
$HASAP_{635}$	VSD	9.3	5	N.A.	N.A.	400	2.1	1.1	656	81,000	0.75	1.811	(Deo et al., 2021)
$Voltron_{525}$	Rhodopsin	-23	-13.5	5[f]	0.5–2.5	400	0.64	0.78	553	83,600	0.87	2.169	(Abdelfattah et al., 2019)
AceD81S-$HaloTag_{TMR}$	Rhodopsin	-19.1	-8.9	11.9	5	484	N.A.	N.A.	574	92,000	0.1	0.274	(Xu et al., 2019)
$Positron_{525}$	Rhodopsin	20	13	5[f]	1.8–6.0	400	0.63	0.64	553	83,600	0.87	2.169	(Abdelfattah et al., 2020)
Flare1-Cy3	Rhodopsin	-35.9	N.A.	n.d	2.4	484	0.92	1.41	569	150,000	0.1	0.447	(Xu et al., 2018)
HVI-Cy3	Rhodopsin	-39.1	-25.3	91.3	2.0–4.9	484	1.7	2.5	569	150,000	0.1	0.447	(Liu et al., 2021)
HVI-Cy5	Rhodopsin	-19.6	-12.8	26.1	0.2–1.2	484	1.87	3.09	670	271,000	0.28	2.262	(Liu et al., 2021)

N.A. not available.
[a] Measured in cultured neurons;
[b] Quantum yield;
[c] Relative brightness, calculated as the product of extinction coefficient and quantum yield, normalized to the brightness of EGFP;
[d] Measured with 525/30 nm excitation filter and a long-pass emission filter (610 nm);
[e] Voltage-dependent redistribution dye;
[f] Measured in vivo.

(Table 1) (Alich et al., 2021).

2.4. Photoinduced electron transfer (PeT) dyes

A PeT dye consists of a fluorescence reporter (e.g. fluorescein), an electron donor (e.g. aniline), and a molecular wire (e.g. alternating single and double bonds) connecting the two moieties. When added to cells, the hydrophobic molecular wire and electron donor are embedded into the cell membrane, while the negatively charged fluorescence reporter is localized at the outer leaflet of the lipid bilayer. When the fluorophore is excited with light illumination, electronic transition would leave a vacant orbital in the ground state, which is then rapidly occupied by an electron that travels through the molecular wire from the aniline moiety. When this photo-induced electron transfer (PeT) process occurs, the electronic ground state becomes fully occupied, thereby decreasing fluorescence emission by preventing electronic transition from the excited state. At resting membrane potential, the transmembrane electric field favors the movement of electrons towards the fluorophore, thus decreasing the fluorescence quantum yield. When the cell is depolarized, the electric field weakens PeT effect and increases the

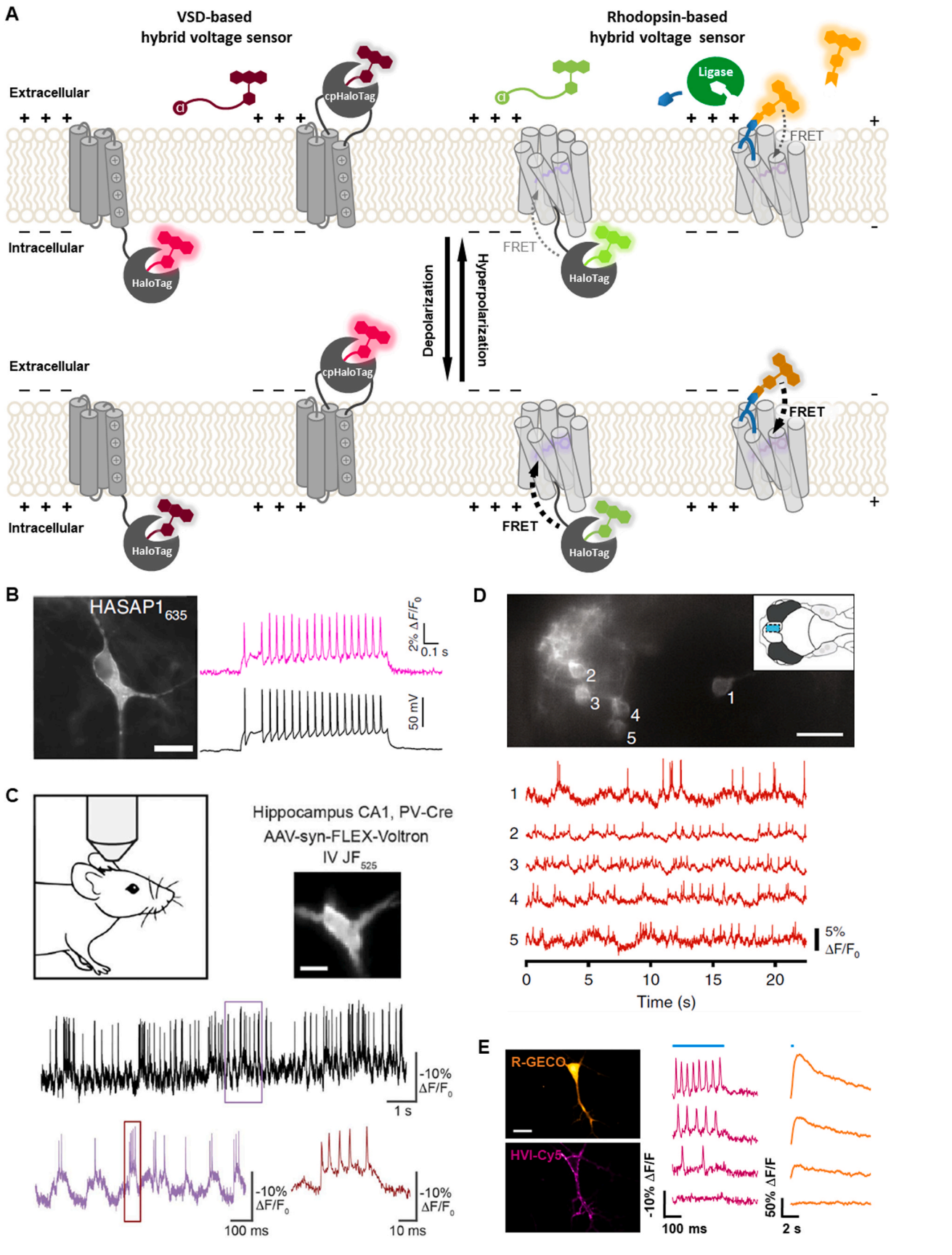

(caption on next page)

Fig. 3. GEVI-derived hybrid voltage sensors. (A) Voltage sensing mechanisms of GEVI-derived hybrid sensors. From left to right: 1) VSD-based hybrid voltage sensors. Voltage dependent conformational change in the VSD perturbs the chemical environment of the HaloTag-targeted fluorophore, thereby changing its fluorescence emission intensity. 2) Rhodopsin-based hybrid voltage sensor. A fluorescence donor is appended to the rhodopsin quencher through either HaloTag or PRIME. As membrane potential changes, electrochromic effect in the rhodopsin modulates the FRET quenching efficiency, thus changing the fluorophore emission. (B) Near-infrared sensor, HASAP1 indicated action potentials in a cultured neuron (Deo et al., 2021). (C) Voltron-JF_{525} was used to long-term monitor the activity of hippocampus PV neurons (Abdelfattah et al., 2019). (D) A voltage sensor with positive-going fluorescence response, Positron indicated action potentials in a zebrafish (Abdelfattah et al., 2020). (E) Another Near-infrared sensor, HVI-Cy5 indicated action potentials in a cultured neuron, and co-image with a red-shifted calcium sensor (Liu et al., 2021).

brightness of the fluorophore (Fig. 2B). The longer the molecular wire and the better it aligns with the transmembrane electric field, the higher voltage sensitivity (Kulkarni and Miller, 2017). Since the time scale by which PeT occurs is far shorter than the nanosecond-scale fluorescence lifetime, PeT OVSDs has fast voltage sensing kinetics.

The first generation of PeT OVSD, VoltageFluor2.1. Cl (VF2.1. Cl), was designed by Miller and co-workers. VF2.1. Cl emits yellow fluorescence with a linear response to voltage changes at a sensitivity of 27% $\Delta F/F_0$ per 100 mV, while no significant changes on neuronal electrophysiology was observed (Miller et al., 2012). Since then, Miller and co-workers have created a series of VF dyes that span the spectrum from green to near-infrared (Woodford et al., 2015; Deal et al., 2016; Huang et al., 2015). Meanwhile, hybrid voltage sensors based on VF dyes were also developed. VF-EX (Voltage-Fluor targeted by esterase expression) uses an enzymatic uncaging strategy to allow voltage imaging in defined neurons (Liu et al., 2017). Initially protected in the form of an acetoxymethyl ether, fluorescence emission from VF-EX is blocked. When the VF-EX precursor is incubated with neurons expressing porcine liver esterase on the cell membrane, the protecting group is removed, thus locally restoring fluorescence. VF-EX 2 exhibits a sensitivity of $21 \pm 0.3\%$ $\Delta F/F_0$ per 100 mV in targeted cells (Table 1).

The enzymatic decaging strategy could be extended to other PeT dyes. For incidence, carboVF-EX was developed by replacing the fluorescein reporter with carbofluorescein (e.g. carboVF2.1(OMe). Cl). The resulting carboVF-EX 1 has an emission peak of 593 nm, which is ~50 nm red-shifted relative to fluorescein. CarboVF-EX 1 reports AP with a sensitivity of 8.4% $\Delta F/F_0$ (Table 1), which is higher than VF-EX 2 but lower than carboVF2.1(OMe). Cl itself ($14 \pm 1\%$ $\Delta F/F_0$ per AP). It is likely that background staining of carboVF-EX 1 has reduced its voltage sensitivity (Ortiz et al., 2019).

An alternative strategy is to target VF dyes with self-labeling protein tags. VoltageSpy is a sarcosine modified VF dye conjugated with a 13-amino-acid peptide SpyTag, which specifically reacts with cell membrane-localized SpyCatcher to form an isopeptide linkage (Zakeri et al., 2012). Through spacer optimization, VoltageSpy 22 (PEG_{35}) could detect evoked APs with a sensitivity of 9.7% $\Delta F/F_0$ per AP (Table 1) and has been used to image subcellular (e.g. axons and dendrites) voltage dynamics in cultured neurons (Grenier et al., 2019). Similarly, RhoVR-Halos was developed by conjugating RhoVR (Deal et al., 2016) (Rhodamine-based Voltage Reporters) with HaloTag (Los et al., 2008) ligand, which specifically reacts with cell membrane-localized HaloTag. RhoVR1-PEG_{25}-Halo exhibits a sensitivity of 11.1% $\Delta F/F_0$ per AP in cultured neurons (Table 1). Furthermore, RhoVR1-PEG_{25}-Halo was applied to image in cortical layer 2/3 of mouse brain slices under 860 nm two-photon illumination and showed a sensitivity of 4.3% per AP (Deal et al., 2020) (Fig. 2D). Recently, the HaloTag method has been extended to BeRST 1 (Berkeley Red Sensor of Transmembrane potential 1), a silicon-rhodamine-based voltage sensor that emits in the far-red (> 650 nm) spectrum. The resulting isoBeRST-Halo 7 has a voltage sensitivity of 10% $\Delta F/F_0$ per AP in cultured neurons (Table 1) and 3.3% $\Delta F/F_0$ per AP in mouse brain slices (Ortiz et al., 2020).

3. GEVI-derived hybrid voltage sensors

Genetically encoded voltage indicators (GEVIs) can be readily targeted to specified neurons, but their photophysical properties are generally inferior to synthetic dyes. Voltage sensitivity of GEVIs arise from either voltage-driven conformational changes in the voltage-sensitive domain (VSD) (Jin et al., 2012; St-Pierre et al., 2014; Villette et al., 2019) or the voltage-dependent chemical equilibrium of microbial rhodopsins (Xu et al., 2019; Hochbaum et al., 2014; Gong et al., 2015; Zou et al., 2014; Piatkevich et al., 2019; Kannan et al., 2018).

3.1. VSD-based GEVIs

The VSD of voltage-sensing phosphatase from *Ciona intestinalis* (Ci-VSD) contains four transmembrane helices, designated as S1 to S4. Due to the presence of positively charged amino acid residues, the S4 helix would shift its position in response to changes in the transmembrane electric field, thus causing conformational changes in the VSD. This structural feature has been leveraged to construct a series of GEVIs by fusing FPs to N- or C-terminus of VSD. For example, as a CiVSD-super ecliptic pHluorin fusion, ArcLight exhibits high sensitivity (~35% $\Delta F/F_0$ per 100 mV) but suffers from slow kinetics (response time constant $\tau = \sim 10$ ms) (Jin et al., 2012). Voltage-induced conformational change of VSD could also be harnessed by inserting an engineered fluorescent protein to the loop connecting S3 and S4. In 2014, a circularly permuted GFP (cpGFP) was inserted to the VSD from chicken voltage sensitive phosphatase to create a faster voltage indicator, termed ASAP1 (Accelerated Sensor of Action Potentials 1). The latest version, ASAP3 has achieved a voltage sensitivity of $-51 \pm 1\%$ $\Delta F/F_0$ per 100 mV and has been applied to report subthreshold potentials and spontaneous APs in anesthetic mice under two-photon microscopy (Villette et al., 2019).

To further enhance the brightness and photostability of VSD-based GEVIs, the FP was replaced by HaloTag (Fig. 3A). Initial effort that used tetramethylrhodamine (TMR) to label HaloTag fused to the C- or N-terminus of CiVSD achieved a modest sensitivity of -2% $\Delta F/F_0$ per 100 mV (Table 1) (Tsutsui et al., 2013). The dynamic range could be greatly enhanced by using dyes that are more sensitive to the chemical environment of HaloTag. For example, the lactone-zwitterionic (L-Z) equilibrium of Janelia Fluor 635 (JF_{635}) dye is affected by electrostatic interactions and local hydrophobicity. When the dye is tethered to HaloTag fused to the C-terminus of CiVSD, voltage-induced conformational changes in the VSD would perturb the local environment of JF_{635} and alters its absorption spectrum by shifting the L-Z equilibrium. This hybrid sensor, called HArcLight, showed $-3.5 \pm 0.2\%$ $\Delta F/F_0$ sensitivity per 100 mV and fast response for reporting APs (-3% $\Delta F/F_0$ per AP) in cultured rat hippocampal neurons (Table 1) (Deo et al., 2021). Similarly, HASAP1 was developed by replacing the cpGFP in ASAP1 with a circularly permutated HaloTag (cpHaloTag) (Fig. 3B) (Deo et al., 2021). HASAP1 exhibits a sensitivity of 5% $\Delta F/F_0$ per AP in cultured rat hippocampal neurons (Table 1).

3.2. Rhodopsin-based GEVIs

Microbial rhodopsins have been widely used as optogenetic actuators, including photo-sensitive channels and pumps (Zhang et al., 2011). In 2011, Cohen and co-workers reported the first voltage-sensing phenomenon in the proton-pumping proteorhodopsin mutant, named PROPS, which they used to investigate electrical spiking in *E. coli* (Kralj et al., 2011). Since this seminal work, more proton-pumping rhodopsins have been developed into GEVIs, including Arch, QuasAr series (Adam et al., 2019; Hochbaum et al., 2014), Archer series (Flytzanis et al., 2014), and Archon series (Piatkevich et al., 2019, 2018). These

rhodopsin-based GEVIs all used the native near infra-red fluorescence of the retinal chromophore that is covalently linked to the protein backbone through a Schiff base. Voltage sensitivity arises from electrochromic effect, in which transmembrane electric field perturbs the reversible protonation/deprotonation chemical equilibrium of the Schiff base, thus affecting the absorption spectrum of the retinal.

Rhodopsin-based GEVIs are characterized with far-red emission spectra and remarkable sensitivity and response kinetics. For example, QuasAr2 has sub-millisecond response kinetics and excellent sensitivity (90% $\Delta F/F_0$ per 100 mV and 48% per AP) (Hochbaum et al., 2014). However, a common drawback of rhodopsin-based GEVIs is their weak fluorescence, which typically requires intense laser illumination at > 100 W/cm^2, more than two orders of magnitude higher than GFP-based indicators (Zou et al., 2014). It is important to note that SNR not only reflects the sensitivity of indicators, but also depends on their expression level and membrane trafficking. Recently, a combination of protein engineering and screening has improved the signal-to-noise ratio (SNR) and molecular brightness of rhodopsin-based GEVIs. For example, the photo-activatable variant of QuasAr2 (i.e. voltage-dependent fluorescence is enhanced by blue light), paQuasAr3 has a voltage sensitivity of ~40% $\Delta F/F_0$ per AP, which is somewhat lower than QuasAr2. Yet, its improved membrane trafficking and expression level compared to QuasAr2, and 2-fold enhanced brightness after photoactivation compared to QuasAr3, have more than offset the loss in dynamic range, ultimately leading to higher SNR (21 ± 12) for APs in brain slices than QuasAr2 (SNR = 16.5). paQuasAr3 has been used to detect APs and subthreshold potential changes in the olfactory bulb and hippocampal neurons in behaving mice (Adam et al., 2019). Soma-localized Archon1 (approximately 2-fold brighter than QuasAr2) (Piatkevich et al., 2018), or SomArchon also successfully reported APs with good SNR (5–15) in the cortex, striatum and hippocampus of awake mice (Piatkevich et al., 2019).

To further enhance molecular brightness, FPs were fused to voltage-sensing rhodopsins as fluorescence reporters. Due the spectral overlap between the FP emission and rhodopsin absorption, electrochromic shift in the rhodopsin absorption spectrum would alter the FRET quenching efficiency between the FP donor and the retinal acceptor. Following this electrochromic FRET (eFRET) strategy, FPs have been fused to QuasAr2 (Zou et al., 2014), Mac (Gong et al., 2014), and Ace2 (Gong et al., 2015) rhodopsin mutants to create a palette of bright GEVIs. For example, Ace2N-mNeon (Gong et al., 2015), a fusion between mNeonGreen and Ace2 rhodopsin from *Acetabularia acetabulum*, has a sensitivity of − 18% $\Delta F/F_0$ per 100 mV, and has been applied to voltage imaging in awake mice and fruit flies (Gong et al., 2015). More recently, red-shifted variants have been created by fusing mOrange2 or mRuby3/4 to Ace2 (D81S) mutant (Xu et al., 2019; Kannan et al., 2018). The Ace2 (D81S)-mRuby3 fusion, VARNAM, could report membrane potential in freely moving mice (Kannan et al., 2018). The Ace2(D81S)-mOrange2 fusion has ~50% higher voltage sensitivity (− 25.9% $\Delta F/F_0$ per 100 mV) than Ace2N-mNeon, due to better spectral overlap (Xu et al., 2019).

While rhodopsin-FP fusions have the advantage of being readily targetable to specified cell subtypes, FPs have several inherent limitations as fluorescence reporters. FPs are typically less bright than synthetic fluorophore and more prone to photobleaching. Their fluorescence emission spectra are often limited to green and red, whereas many far-red and even infra-red dyes are commercially available. To overcome the above limitations of rhodopsin-FP GEVIs, hybrid chemigenetic indicators were created by using organic dyes with higher photostability and brightness as reporters instead of FPs. This strategy requires highly biocompatible and site-specific protein conjugation techniques to create the desired rhodopsin-dye linkage. Voltron (Abdelfattah et al., 2019) was created by fusing Ace2 rhodopsin mutant with HaloTag, which subsequently binds to its cognate ligand conjugated with a fluorophore (Fig. 3A) (Los et al., 2008). Recently developed Janelia Fluor dyes (Grimm et al., 2017) could pass through the blood brain barrier, thus enabling voltage imaging in vivo. The high photostability of JF_{525}, for example, has allowed Voltron to continuously report membrane potential dynamics in L1 neurons in the visual cortex for 15 min, with good SNR (4–5) at low illumination power density (0.3–2 W/cm^2) (Fig. 3C and Table 1) (Abdelfattah et al., 2019). This strategy could be readily extended to other self-labeling protein tags, including SNAP-tag (Xu et al., 2019). Further engineering of Ace2 rhodopsin, with a particular focus on the proton-pumping pathway, has led to the development of hybrid sensors with ~50% improved sensitivity (i.e. Ace(D81S)-HaloTag$_{TMR}$ (Xu et al., 2019)) or positive-going fluorescence response with a sensitivity of 13% $\Delta F/F_0$ per AP (i.e. Positron$_{525}$ (Abdelfattah et al., 2020)) (Fig. 3D and Table 1). Together, these hybrid eFRET sensors have substantially improved brightness compared to their rhodopsin-FP GEVI counterparts, yet their voltage sensitivities are similarly low in terms of $\Delta F/F_0$, which are typically less than 15% for reporting a single neuronal action potential (Xu et al., 2018). According to the eFRET theory, voltage sensitivity is linearly proportional to the baseline FRET efficiency, which is influenced by the spectral overlap, dipole orientation and donor-acceptor distance. In the cases of both rhodopsin-FP GEVIs and rhodopsin-HaloTag chemigenetic indicators, the C-terminally fused bulky protein tags (e.g. FP ~28 kDa (Zou et al., 2014), HaloTag ~34 kDa (Los et al., 2008)) has prevented close contact between the fluorophore donor and the retinal located at the core of the rhodopsin, thus limiting the FRET efficiency. A back-of-the-envelope calculation suggests that, in the shot noise-limited regime, SNR is highest when the baseline FRET efficiency reaches 67%, whereas most FP-based eFRET GEVIs have their baseline FRET efficiencies below 20%. Interested readers are referred to the Supplementary Discussion of reference (Xu et al., 2018).

To improve the FRET efficiency and hence voltage sensitivity, it is important to shorten the distance between retinal and fluorescent reporter. One strategy is to replace bulky protein tags with small peptide tags, which are site-specifically derivatized with chemical fluorophores with small molecular size. This strategy has been implemented in Flare1 (fluorophore ligation-assisted rhodopsin eFRET indicator 1), which utilized PRIME (probe-incorporation mediated by enzyme) and bioorthogonal reaction to construct hybrid voltage indicators (Fig. 3A) (Liu et al., 2012). Site-specific labeling is achieved in two steps: first, a bioorthogonal functional group handle (i.e. picolylazide) is enzymatically ligated to a 13-amino acid peptide (LAP peptide) inserted to the extracellular loop of engineered Ace2 rhodopsin mutant; then, an alkyne-functionalized fluorophore is introduced to the LAP peptide via copper-assisted alkyne-azide cycloaddition (CuAAC) reaction. Insertion of a short peptide rather than a well-folded protein to an internal loop could minimize the unwanted perturbation of membrane protein folding and trafficking. Flare1-Cy3 showed a sensitivity of − 35.9% $\Delta F/F_0$ per 100 mV (Table 1) and was applied to optically map the gap junction-mediated electrical conduction over hundreds of micrometers in HEK293T cells (Xu et al., 2018). By replacing the neural toxic CuAAC reaction with the more biocompatible Diels-Alder reaction and by adopting an Ace2(D81C) mutant with higher sensitivity and red-shifted spectrum, an improved version of hybrid voltage indicator (HVI) was created. HVI achieved high dynamic range ($\Delta F/F_0 = -25.3\%$ per AP for HVI-Cy3), especially in the far-red spectrum ($\Delta F/F_0 = -12.8\%$ per AP for HVI-Cy5) (Table 1). HVI-Cy5 could be paired with optogenetic actuators and green/red-emitting fluorescent indicators, allowing multiplexed imaging and all-optical electrophysiology in cultured neurons (Fig. 3E) (Liu et al., 2021).

4. Summary

In this mini-review, we briefly summarized the history of hybrid voltage sensor development, focusing on the voltage sensing mechanism and the structural design. From the mechanistic point of view, hybrid sensors are created either by conjugating organic voltage-sensing dyes (OVSDs) to protein scaffolds or by modifying genetically encoded

voltage indicators (GEVIs) with dye reporters. In OVSD-derived hybrid indicators, the dye itself is both the voltage sensor and the fluorescence reporter, while the protein scaffold functions as a cell-specific anchor. To achieve high voltage sensitivity and high SNR, one has to battle against undesired non-discriminative staining in the sample, as any off-target fluorophore would contribute to the background and noise, thus corroding the sensitivity and SNR. In comparison, GEVI-derived hybrid indicators are more modular in design: the membrane protein scaffold senses the transmembrane electric field, while the synthetic dye acts merely as the fluorescence reporter. There must exist a transmission mechanism that harnesses voltage-dependent conformational changes (i.e. in VSDs) or chemical equilibrium shifts (i.e. in rhodopsins) to drive changes in fluorescence emission intensities. Therefore, optimizing the transmission efficiency is of paramount importance for GEVI-derived hybrid indicators.

From the structural point of view, most hybrid sensors (with the exception of hVOS series) are characterized by the covalent linkage between a protein scaffold and a synthetic dye molecule. At the core of this design is the highly biocompatible chemical ligation reaction that occurs in the context of live neurons or brain tissues. Over the past decades, efforts in the chemical biology community have created an arsenal of bioorthogonal reactions (e.g. inverse electron demand Diels-Alder reaction), engineered enzymes (e.g. bacterial lipoate protein ligase, porcine liver esterase), and self-labeling protein tags (e.g. HaloTag, SpyCatcher). These tools offer the site-specific precision and fast reaction kinetics that are indispensable for constructing hybrid sensors. Future development of hybrid voltage sensors would continue to benefit from the ever-expanding toolbox of ligation methods, including smaller and more efficient self-labeling protein tags, evolved and/or computationally designed enzymes, and newly discovered bioorthogonal reactions.

Two challenges exist for future development of hybrid indicators. One is reagent delivery into the mammalian brain for in vivo imaging. In this respect, several HaloTag ligand-conjugated JF dyes have the advantage of being able to cross blood-brain barrier, so that when injected into orbital sinus, they could reach their HaloTag targets in the brain (Abdelfattah et al., 2019; Grimm et al., 2017). In comparison, HVI-Cy5 requires exogenous addition of a 37 kDa enzyme which could not be delivered in the same way as the JF dyes. Another challenge is the internalization of transmembrane protein scaffolds, which determines the duration of time in which the fluorescence label remains on the cell surface. Unlike GEVIs which are continually delivered to the plasma membrane through secretory pathway, hybrid indicators are assembled in situ during a short time window, after which they are slowly yet inevitably turned over due to endocytosis.

The other challenge is phototoxicity that is often associated with synthetic dyes. Phototoxicity typically arises from photochemical processes that lead to the production of reactive oxygen species (ROS), which oxidizes and inactivates neighboring biomolecules. This is exacerbated by a starvation for photons during kilo-Hertz voltage imaging, which necessitates high illumination power to achieve high SNR. Fluorophores with less phototoxicity are highly sought after. Recently developed Janelia Fluor dye series, such as JF549 and JF525, are bright and require lower illumination intensity (Gong et al., 2014). Imaging with far red fluorophores (e.g. HTL-JF635 and cy5 was used well with HASAP1 and HVI) are also advantageous as their long excitation wavelengths are not matched to the excitation peak of riboflavin molecules (peak = 443 and 353 nm), which are native photosensitizers in the cellular environment. Therefore, hybrid voltage sensors would greatly benefit from the development of fluorophores with higher extinction coefficients, higher quantum yields, better photo-stability and more red-shifted spectra, all of which would contribute to achieving higher SNR with lower illumination power, thus reduced cellular phototoxicity.

Overall, by harnessing the power of both chemistry and biology, hybrid voltage sensors have complemented existing OVSDs and GEVIs to achieve higher sensitivity, faster kinetics and more red-shifted spectrum (Fig. 4). While this hybrid strategy still faces several challenges associated with in vivo imaging, we envision that these problems may be eventually solved through coordinated efforts of protein engineering, chemical synthesis, high-throughput screening in the future.

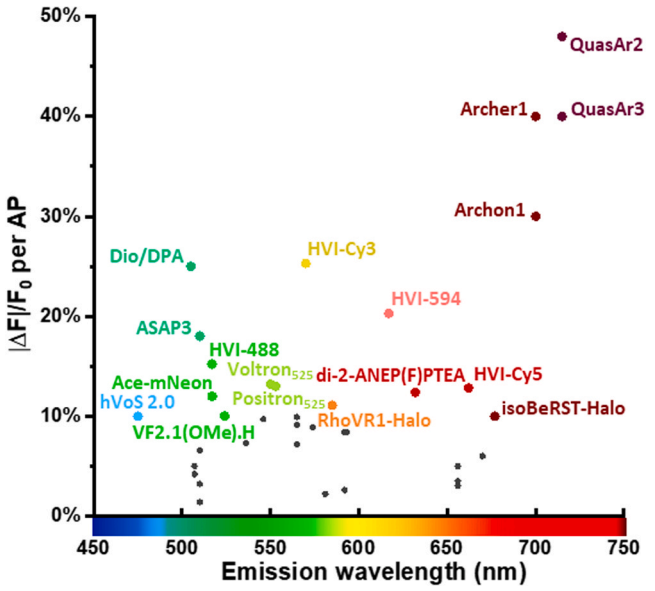

Fig. 4. Plot of fluorophore emission wavelength (nm) versus the absolute sensitivity ($|\Delta F|/F_0$ per action potential) for several representative voltage indicators. The color of the name indicates its wavelength of maximum emission (λ_{em}).

Declaration of Competing Interest

The authors declare no competing financial interests.

Acknowledgements

We acknowledge funding from the Ministry of Science and Technology (2018YFA0507600 and 2017YFA0503600), the National Natural Science Foundation of China (21727806 and 32088101). PZ is sponsored by Li Ge-Zhao Ning Life Science Junior Research Fellowship and Bayer Investigator Award.

References

Abdelfattah, A.S., Kawashima, T., Singh, A., Novak, O., Liu, H., Shuai, Y., Huang, Y.C., Campagnola, L., Seeman, S.C., Yu, J., Zheng, J., Grimm, J.B., Patel, R., Friedrich, J., Mensh, B.D., Paninski, L., Macklin, J.J., Murphy, G.J., Podgorski, K., Lin, B.J., Chen, T.W., Turner, G.C., Liu, Z., Koyama, M., Svoboda, K., Ahrens, M.B., Lavis, L.D., Schreiter, E.R., 2019. Bright and photostable chemigenetic indicators for extended in vivo voltage imaging. Science 365, 699–704.

Abdelfattah, A.S., et al., 2020. A general approach to engineer positive-going eFRET voltage indicators. Nat. Commun. 11, 3444.

Adam, Y., Kim, J.J., Lou, S., Zhao, Y., Xie, M.E., Brinks, D., Wu, H., Mostajo-Radji, M.A., Kheifets, S., Parot, V., Chettih, S., Williams, K.J., Gmeiner, B., Farhi, S.L., Madisen, L., Buchanan, E.K., Kinsella, I., Zhou, D., Paninski, L., Harvey, C.D., Zeng, H., Arlotta, P., Campbell, R.E., Cohen, A.E., 2019. Voltage imaging and optogenetics reveal behaviour-dependent changes in hippocampal dynamics. Nature 569, 413–417.

Alich, T.C., Pabst, M., Pothmann, L., Szalontai, B., Faas, G.C., Mody, I., 2021. A dark quencher genetically encodable voltage indicator (dqGEVI) exhibits high fidelity and speed. Proc. Natl. Acad. Sci. USA 118.

Bayguinov, P.O., Ma, Y., Gao, Y., Zhao, X., Jackson, M.B., 2017. Imaging voltage in genetically defined neuronal subpopulations with a Cre Recombinase-targeted hybrid voltage sensor. J. Neurosci. 37, 9305–9319.

Bradley, J., Luo, R., Otis, T.S., DiGregorio, D.A., 2009. Submillisecond optical reporting of membrane potential in situ using a neuronal tracer dye. J. Neurosci. 29, 9197–9209.

Chanda, B., Blunck, R., Faria, L.C., Schweizer, F.E., Mody, I., Bezanilla, F., 2005. A hybrid approach to measuring electrical activity in genetically specified neurons. Nat. Neurosci. 8, 1619–1626.
Davila, H.V., Salzberg, B.M., Cohen, L.B., Waggoner, A.S., 1973. A large change in axon fluorescence that provides a promising method for measuring membrane potential. Nat. New Biol. 241, 159–160.
Deal, P.E., Liu, P., Al-Abdullatif, S.H., Muller, V.R., Shamardani, K., Adesnik, H., Miller, E.W., 2020. Covalently tethered rhodamine voltage reporters for high speed functional imaging in brain tissue. J. Am. Chem. Soc. 142, 614–622.
Deal, P.E., Kulkarni, R.U., Al-Abdullatif, S.H., Miller, E.W., 2016. Isomerically pure tetramethylrhodamine voltage reporters. J. Am. Chem. Soc. 138, 9085–9088.
Deo, C., Abdelfattah, A.S., Bhargava, H.K., Berro, A.J., Falco, N., Farrants, H., Moeyaert, B., Chupanova, M., Lavis, L.D., Schreiter, E.R., 2021. The HaloTag as a general scaffold for far-red tunable chemigenetic indicators. Nat. Chem. Biol. 17, 718–723.
Fluhler, E., Burnham, V.G., Loew, L.M., 1985. Spectra, membrane binding, and potentiometric responses of new charge shift probes. Biochemistry 24, 5749–5755.
Flytzanis, N.C., Bedbrook, C.N., Chiu, H., Engqvist, M.K., Xiao, C., Chan, K.Y., Sternberg, P.W., Arnold, F.H., Gradinaru, V., 2014. Archaerhodopsin variants with enhanced voltage-sensitive fluorescence in mammalian and Caenorhabditis elegans neurons. Nat. Commun. 5, 4894.
Gong, Y., Huang, C., Li, J.Z., Grewe, B.F., Zhang, Y., Eismann, S., Schnitzer, M.J., 2015. High-speed recording of neural spikes in awake mice and flies with a fluorescent voltage sensor. Science 350, 1361–1366.
Gong, Y., Wagner, M.J., Zhong Li, J., Schnitzer, M.J., 2014. Imaging neural spiking in brain tissue using FRET-opsin protein voltage sensors. Nat. Commun. 5, 3674.
Gonzalez, J.E., Tsien, R.Y., 1997. Improved indicators of cell membrane potential that use fluorescence resonance energy transfer. Chem. Biol. 4, 269–277.
Grenier, V., Daws, B.R., Liu, P., Miller, E.W., 2019. Spying on neuronal membrane potential with genetically targetable voltage indicators. J. Am. Chem. Soc. 141, 1349–1358.
Grimm, J.B., Muthusamy, A.K., Liang, Y., Brown, T.A., Lemon, W.C., Patel, R., Lu, R., Macklin, J.J., Keller, P.J., Ji, N., Lavis, L.D., 2017. A general method to fine-tune fluorophores for live-cell and in vivo imaging. Nat. Methods 14, 987–994.
Hochbaum, D.R., Zhao, Y., Farhi, S.L., Klapoetke, N., Werley, C.A., Kapoor, V., Zou, P., Kralj, J.M., Maclaurin, D., Smedemark-Margulies, N., Saulnier, J.L., Boulting, G.L., Straub, C., Cho, Y.K., Melkonian, M., Wong, G.K., Harrison, D.J., Murthy, V.N., Sabatini, B.L., Boyden, E.S., Campbell, R.E., Cohen, A.E., 2014. All-optical electrophysiology in mammalian neurons using engineered microbial rhodopsins. Nat. Methods 11, 825–833.
Huang, Y.L., Walker, A.S., Miller, E.W., 2015. A photostable silicon rhodamine platform for optical voltage sensing. J. Am. Chem. Soc. 137, 10767–10776.
Jin, L., Han, Z., Platisa, J., Wooltorton, J.R., Cohen, L.B., Pieribone, V.A., 2012. Single action potentials and subthreshold electrical events imaged in neurons with a fluorescent protein voltage probe. Neuron 75, 779–785.
Kannan, M., Vasan, G., Huang, C., Haziza, S., Li, J.Z., Inan, H., Schnitzer, M.J., Pieribone, V.A., 2018. Fast, in vivo voltage imaging using a red fluorescent indicator. Nat. Methods 15, 1108–1116.
Kralj, J.M., Hochbaum, D.R., Douglass, A.D., Cohen, A.E., 2011. Electrical spiking in Escherichia coli probed with a fluorescent voltage-indicating protein. Science 333, 345–348.
Kulkarni, R.U., Miller, E.W., 2017. Voltage imaging: pitfalls and potential. Biochemistry 56, 5171–5177.
Lavis, L.D., Raines, R.T., 2008. Bright ideas for chemical biology. ACS Chem. Biol. 3, 142–155.
Lazzari-Dean, J.R., Gest, A.M.M., Miller, E.W., 2021. Measuring absolute membrane potential across space and time. Annu. Rev. Biophys. 50, 447–468.
Liu, P., Grenier, V., Hong, W., Muller, V.R., Miller, E.W., 2017. Fluorogenic targeting of voltage-sensitive dyes to neurons. J. Am. Chem. Soc. 139, 17334–17340.
Liu, S., Lin, C., Xu, Y., Luo, H., Peng, L., Zeng, X., Zheng, H., Chen, P.R., Zou, P., 2021. A far-red hybrid voltage indicator enabled by bioorthogonal engineering of rhodopsin on live neurons. Nat. Chem. 13, 472–479.
Liu, D.S., Tangpeerachaikul, A., Selvaraj, R., Taylor, M.T., Fox, J.M., Ting, A.Y., 2012. Diels-Alder cycloaddition for fluorophore targeting to specific proteins inside living cells. J. Am. Chem. Soc. 134, 792–795.
Los, G.V., Encell, L.P., McDougall, M.G., Hartzell, D.D., Karassina, N., Zimprich, C., Wood, M.G., Learish, R., Ohana, R.F., Urh, M., Simpson, D., Mendez, J., Zimmerman, K., Otto, P., Vidugiris, G., Zhu, J., Darzins, A., Klaubert, D.H., Bulleit, R. F., Wood, K.V., 2008. HaloTag: a novel protein labeling technology for cell imaging and protein analysis. ACS Chem. Biol. 3, 373–382.
Miller, E.W., 2016. Small molecule fluorescent voltage indicators for studying membrane potential. Curr. Opin. Chem. Biol. 33, 74–80.
Miller, E.W., Lin, J.Y., Frady, E.P., Steinbach, P.A., Kristan WB, Jr, Tsien, R.Y., 2012. Optically monitoring voltage in neurons by photo-induced electron transfer through molecular wires. Proc. Natl. Acad. Sci. USA 109, 2114–2119.
Ng, D.N., Fromherz, P., 2011. Genetic targeting of a voltage-sensitive dye by enzymatic activation of phosphonooxymethyl-ammonium derivative. ACS Chem. Biol. 6, 444–451.
Ortiz, G., Liu, P., Naing, S.H.H., Muller, V.R., Miller, E.W., 2019. Synthesis of sulfonated carbofluoresceins for voltage imaging. J. Am. Chem. Soc. 141, 6631–6638.
Ortiz, G.L., Pei, Deal, Parker, Nensel, Ashley, Martinez, Kayli, Shamardani, Kiarash, et al., 2020. A silicon-rhodamine chemical-genetic hybrid for far red voltage imaging from defined neurons in brain slice. ChemRxiv.
Piatkevich, K.D., Bensussen, S., Tseng, H.A., Shroff, S.N., Lopez-Huerta, V.G., Park, D., Jung, E.E., Shemesh, O.A., Straub, C., Gritton, H.J., Romano, M.F., Costa, E., Sabatini, B.L., Fu, Z., Boyden, E.S., Han, X., 2019. Population imaging of neural activity in awake behaving mice. Nature 574, 413–417.
Piatkevich, K.D., Jung, E.E., Straub, C., Linghu, C., Park, D., Suk, H.J., Hochbaum, D.R., Goodwin, D., Pnevmatikakis, E., Pak, N., Kawashima, T., Yang, C.T., Rhoades, J.L., Shemesh, O., Asano, S., Yoon, Y.G., Freifeld, L., Saulnier, J.L., Riegler, C., Engert, F., Hughes, T., Drobizhev, M., Szabo, B., Ahrens, M.B., Flavell, S.W., Sabatini, B.L., Boyden, E.S., 2018. A robotic multidimensional directed evolution approach applied to fluorescent voltage reporters. Nat. Chem. Biol. 14, 352–360.
Shahrjerdi, D., Bedell, S.W., 2013. Extremely flexible nanoscale ultrathin body silicon integrated circuits on plastic. Nano Lett. 13, 315–320.
Sjulson, L., Miesenbock, G., 2008. Rational optimization and imaging in vivo of a genetically encoded optical voltage reporter. J. Neurosci. 28, 5582–5593.
St-Pierre, F., Marshall, J.D., Yang, Y., Gong, Y., Schnitzer, M.J., Lin, M.Z., 2014. High-fidelity optical reporting of neuronal electrical activity with an ultrafast fluorescent voltage sensor. Nat. Neurosci. 17, 884–889.
Steinmetz, N.A., Aydin, C., Lebedeva, A., Okun, M., Pachitariu, M., Bauza, M., Beau, M., Bhagat, J., Böhm, C., Broux, M., Chen, S., Colonell, J., Gardner, R.J., Karsh, B., Kloosterman, F., Kostadinov, D., Mora-Lopez, C., O'Callaghan, J., Park, J., Putzeys, J., Sauerbrei, B., van Daal, R., Vollan, A.Z., Wang, S., Welkenhuysen, M., Ye, Z., Dudman, J.T., Dutta, B., Hantman, A.W., Harris, K.D., Lee, A.K., Moser, E.I., O'Keefe, J., Renart, A., Svoboda, K., Häusser, M., Haesler, S., Carandini, M., Harris, T.D., 2021. Neuropixels 2.0: a miniaturized high-density probe for stable, long-term brain recordings. Science 372.
Sundukova, M., Prifti, E., Bucci, A., Kirillova, K., Serrao, J., Reymond, L., Umebayashi, M., Hovius, R., Riezman, H., Johnsson, K., Heppenstall, P.A., 2019. A chemogenetic approach for the optical monitoring of voltage in neurons. Angew. Chem. Int. Ed. Engl. 58, 2341–2344.
Tsutsui, H., Jinno, Y., Tomita, A., Okamura, Y., 2013. Optically detected structural change in the N-terminal region of the voltage-sensor domain. Biophys. J. 105, 108–115.
Villette, V., Chavarha, M., Dimov, I.K., Bradley, J., Pradhan, L., Mathieu, B., Evans, S.W., Chamberland, S., Shi, D., Yang, R., Kim, B.B., Ayon, A., Jalil, A., St-Pierre, F., Schnitzer, M.J., Bi, G., Toth, K., Ding, J., Dieudonné, S., Lin, M.Z., 2019. Ultrafast two-photon imaging of a high-gain voltage indicator in awake behaving mice. Cell 179 (1590–1608), 1590–1608.
Wang, A., Feng, J., Li, Y., Zou, P., 2018. Beyond fluorescent proteins: hybrid and bioluminescent indicators for imaging neural activities. ACS Chem. Neurosci. 9, 639–650.
Wang, D., Zhang, Z., Chanda, B., Jackson, M.B., 2010. Improved probes for hybrid voltage sensor imaging. Biophys. J. 99, 2355–2365.
Woodford, C.R., Frady, E.P., Smith, R.S., Morey, B., Canzi, G., Palida, S.F., Araneda, R.C., Kristan WB, Jr, Kubiak, C.P., Miller, E.W., Tsien, R.Y., 2015. Improved PeT molecules for optically sensing voltage in neurons. J. Am. Chem. Soc. 137, 1817–1824.
Xu, Y., Deng, M., Zhang, S., Yang, J., Peng, L., Chu, J., Zou, P., 2019. Imaging neuronal activity with fast and sensitive red-shifted electrochromic FRET indicators. ACS Chem. Neurosci. 10, 4768–4775.
Xu, Y., Peng, L., Wang, S., Wang, A., Ma, R., Zhou, Y., Yang, J., Sun, D.E., Lin, W., Chen, X., Zou, P., 2018. Hybrid indicators for fast and sensitive voltage imaging. Angew. Chem. Int. Ed. Engl. 57, 3949–3953.
Yan, P., Acker, C.D., Zhou, W.L., Lee, P., Bollensdorff, C., Negrean, A., Lotti, J., Sacconi, L., Antic, S.D., Kohl, P., Mansvelder, H.D., Pavone, F.S., Loew, L.M., 2012. Palette of fluorinated voltage-sensitive hemicyanine dyes. Proc. Natl. Acad. Sci. USA 109, 20443–20448.
Zakeri, B., Fierer, J.O., Celik, E., Chittock, E.C., Schwarz-Linek, U., Moy, V.T., Howarth, M., 2012. Peptide tag forming a rapid covalent bond to a protein, through engineering a bacterial adhesin. Proc. Natl. Acad. Sci. USA 109, E690–697.
Zhang, F., Vierock, J., Yizhar, O., Fenno, L.E., Tsunoda, S., Kianianmomeni, A., Prigge, M., Berndt, A., Cushman, J., Polle, J., Magnuson, J., Hegemann, P., Deisseroth, K., 2011. The microbial opsin family of optogenetic tools. Cell 147, 1446–1457.
Zou, P., Zhao, Y., Douglass, A.D., Hochbaum, D.R., Brinks, D., Werley, C.A., Harrison, D. J., Campbell, R.E., Cohen, A.E., 2014. Bright and fast multicoloured voltage reporters via electrochromic FRET. Nat. Commun. 5, 4625.